

Notes on Numerical Fluid Mechanics  
and Multidisciplinary Design 149

Michel Deville · Christophe Calvin ·  
Vincent Couaillier ·  
Marta De La Llave Plata ·  
Jean-Luc Estivalèzes · Thiên Hiệp Lê ·  
Stéphane Vincent *Editors*

# Turbulence and Interactions

Proceedings of the TI 2018 Conference,  
June 25–29, 2018, Les Trois-Îlets,  
Martinique, France

 Springer

# **Notes on Numerical Fluid Mechanics and Multidisciplinary Design**

Volume 149

## **Founding Editor**

Ernst Heinrich Hirschel, Zorneding, Germany

## **Series Editor**

Wolfgang Schröder, Aerodynamisches Institut, RWTH Aachen, Aachen, Germany

## **Editorial Board Members**

Bendiks Jan Boersma, Delft University of Technology, Delft, The Netherlands

Kozo Fujii, Institute of Space & Astronautical Science (ISAS), Sagamihara,  
Kanagawa, Japan

Werner Haase, Hohenbrunn, Germany

Michael A. Leschziner, Department of Aeronautics, Imperial College, London, UK

Jacques Periaux, Paris, France

Sergio Pirozzoli, Department of Mechanical and Aerospace Engineering,  
University of Rome 'La Sapienza', Roma, Italy

Arthur Rizzi, Department of Aeronautics, KTH Royal Institute of Technology,  
Stockholm, Sweden

Bernard Roux, Ecole Supérieure d'Ingénieurs de Marseille, Marseille CX 20,  
France

Yurii I. Shokin, Siberian Branch of the Russian Academy of Sciences, Novosibirsk,  
Russia

## **Managing Editor**

Esther Mäteling, RWTH Aachen University, Aachen, Germany

Notes on Numerical Fluid Mechanics and Multidisciplinary Design publishes state-of-art methods (including high performance methods) for numerical fluid mechanics, numerical simulation and multidisciplinary design optimization. The series includes proceedings of specialized conferences and workshops, as well as relevant project reports and monographs.

More information about this series at <http://www.springer.com/series/4629>

Michel Deville · Christophe Calvin ·  
Vincent Couaillier · Marta De La Llave Plata ·  
Jean-Luc Estivalèzes · Thiên Hiệp Lê ·  
Stéphane Vincent  
Editors

# Turbulence and Interactions

Proceedings of the TI 2018 Conference,  
June 25–29, 2018, Les Trois-Îlets,  
Martinique, France

 Springer

*Editors*

Michel Deville  
EPFL-STI-DO  
Lausanne, Vaud, Switzerland

Christophe Calvin  
FR-91191 Gif-sur-Yvette cedex  
CEA/DRF, CEA/Paris-Saclay  
Sainte-Geneviève-des-Bois, France

Vincent Couaillier  
Centre de Châtillon  
ONERA - The French Aerospace Lab  
Châtillon, France

Marta De La Llave Plata  
ONERA Toulouse  
Toulouse Cedex, France

Jean-Luc Estivalèzes  
ONERA Toulouse  
Toulouse Cedex 4, France

Thiên Hiệp Lê  
ONERA Châtillon  
Châtillon Cedex, France

Stéphane Vincent  
MSME Laboratory  
University of Paris-Est  
Champs-sur-Marne, France

ISSN 1612-2909                      ISSN 1860-0824 (electronic)  
Notes on Numerical Fluid Mechanics and Multidisciplinary Design  
ISBN 978-3-030-65819-9              ISBN 978-3-030-65820-5 (eBook)  
<https://doi.org/10.1007/978-3-030-65820-5>

© Springer Nature Switzerland AG 2021

This work is subject to copyright. All rights are reserved by the Publisher, whether the whole or part of the material is concerned, specifically the rights of translation, reprinting, reuse of illustrations, recitation, broadcasting, reproduction on microfilms or in any other physical way, and transmission or information storage and retrieval, electronic adaptation, computer software, or by similar or dissimilar methodology now known or hereafter developed.

The use of general descriptive names, registered names, trademarks, service marks, etc. in this publication does not imply, even in the absence of a specific statement, that such names are exempt from the relevant protective laws and regulations and therefore free for general use.

The publisher, the authors and the editors are safe to assume that the advice and information in this book are believed to be true and accurate at the date of publication. Neither the publisher nor the authors or the editors give a warranty, expressed or implied, with respect to the material contained herein or for any errors or omissions that may have been made. The publisher remains neutral with regard to jurisdictional claims in published maps and institutional affiliations.

This Springer imprint is published by the registered company Springer Nature Switzerland AG  
The registered company address is: Gewerbestrasse 11, 6330 Cham, Switzerland

# Contents

## Keynote Lectures

<b>Fluid-Structure Interactions in Discrete Mechanics</b> . . . . .	3
Jean-Paul Caltagirone and Philippe Angot	
<b>HPC and Data: When Two Becomes One</b> . . . . .	14
Christophe Calvin and France Boillod-Cerneux	
<b>LES of the Flow Past a Circular Cylinder Using a Multiscale Discontinuous Galerkin Method</b> . . . . .	26
Marta de la Llave Plata, Fabio Naddei, and Vincent Couaillier	
<b>A Volume-of-Fluid Dual-Scale Approach for Simulating Turbulent Liquid/Gas Interactions</b> . . . . .	39
Dominic Kedelty, James Uglietta, and Marcus Herrmann	
<b>Influence of Particle Anisotropy and Motility on Preferential Concentration in Turbulence</b> . . . . .	52
Cristian Marchioli, Harshit Bhatia, and Diego Dotto	
<b>Reference Solutions and URANS Model Characterization for Turbulent Forced Convection Around Heated Square Cylinders</b> . . .	66
Xavier Nicolas, Hua Sun, and Yannick Sommerer	
<b>A Convergence Study of the One-Fluid Formulation in a Phase Inversion Application at Moderate Reynolds and Weber Numbers</b> . . . .	80
Taraneh Sayadi, Stéphane Zaleski, Stéphane Popinet, Vincent Le Chenadec, and Stéphane Vincent	
<b>Finite-Volume Filtering in Large-Eddy Simulations Using a Minimum-Dissipation Model</b> . . . . .	91
Roel Verstappen	

## Contributed Papers

<b>Simulation of a Particulate Flow in 3D Using Volume Penalization Methods</b> . . . . .	103
Philippe Angot, Léa Batteux, Jacques Laminie, and Pascal Poullet	
<b>Simulation of a Confined Turbulent Round Jet at Moderate Reynolds Number</b> . . . . .	110
Georges Halim Atallah, Emmanuel Belut, Sullivan Lechêne, Benoît Trouette, and Stéphane Vincent	
<b>Effect of Very-Large-Scale Motions on One- and Two-Point Statistics in Turbulent Pipe Flow Investigated by Direct Numerical Simulations</b> . . . . .	117
Christian Bauer and Claus Wagner	
<b>Large Eddy Simulation of Turbulent Heat Transfer in Pipe Flows of Temperature Dependent Power-Law Fluids</b> . . . . .	123
Paulin Sourou Ganmbode, Meryem Ould-Rouiss, Xavier Nicolas, and Paolo Orlandi	
<b>The Flow Around a Surface Combatant at 10° Static Drift: Assessment of Turbulence Models</b> . . . . .	130
Emmanuel Guilmineau, Michel Visonneau, and Ginevra Rubino	
<b>Experiments and Large Eddy Simulations on Particle Interaction with a Turbulent Air Jet Impacting a Wall</b> . . . . .	136
Syphax Ikardouchene, Xavier Nicolas, Stéphane Delaby, and Meryem Ould-Rouiss	
<b>A Review of Geometrical Interface Properties for 3D Front-Tracking Methods</b> . . . . .	144
Désir-André Koffi Bi, Mathilde Tavares, Éric Chénier, and Stéphane Vincent	
<b>Soft-Sphere DEM Simulation of Coarse Particles Transported by a Fully Developed Turbulent Gas Vertical Channel Flow</b> . . . . .	150
Ainur Nigmatova, Yann Dufresne, Enrica Masi, Vincent Moureau, and Olivier Simonin	
<b>Rod-Bundle Thermalhydraulics Mixing Phenomena: 3D Analysis with CATHARE-3 of ROSA-2/LSTF Experiment</b> . . . . .	161
Raphaël Préa and Anouar Mekkas	
<b>Sensitivity of Approximate Deconvolution Model Parameters in a <i>Posteriori</i> LES of Interfacial Turbulence</b> . . . . .	169
Mahdi Saeedipour, Stéphane Vincent, and Stefan Pirker	

**Time-Resolved High-Density Particle Tracking Velocimetry of Turbulent Rayleigh-Bénard Convection in a Cubic Sample** . . . . . 176  
 Daniel Schiepel, Sebastian Herzog, and Claus Wagner

**Sub-grid Deconvolution Approach for Filtered Two-Fluid Models and the Application to Fluidized Gas-Particle Suspensions** . . . . . 183  
 Simon Schneiderbauer and Mahdi Saeedipour

**A Front-Tracking Method for Multiphase Flows with a Sharp Interface Representation** . . . . . 189  
 Mathilde Tavares, Désir-André Koffi Bi, Eric Chénier, and Stéphane Vincent

**Bayesian Estimation of Turbulent Flow Intermittency** . . . . . 196  
 Adaté Tossa, Didier Bernard, and Richard Emilion

**Lagrangian Scheme for Scalar Advection-Diffusion. Application to Pollutant Transport** . . . . . 202  
 Benoît Trouette, Georges Halim Atallah, and Stéphane Vincent

**Spreading Time of Liquid Droplets Impacting on Non-wetting Solid Surfaces** . . . . . 208  
 Yang Xu, Stéphane Vincent, Q.-C. He, and H. Le-Quang

**Author Index** . . . . . 217

# **Keynote Lectures**



# Fluid-Structure Interactions in Discrete Mechanics

Jean-Paul Caltagirone<sup>1</sup> and Philippe Angot<sup>2</sup>(✉)

<sup>1</sup> Institut Ingénierie Mécanique de Bordeaux, Dept. TREFLE, CNRS UMR5295, Université de Bordeaux, 16 Avenue Pey-Berland, 33607 Pessac Cedex, France  
calta@ipb.fr

<sup>2</sup> Institut de Mathématiques de Marseille, CNRS UMR7373, Aix-Marseille Université, Centrale Marseille, 13453 Marseille Cedex, France  
philippe.angot@univ-amu.fr

**Abstract.** The primary objective of discrete mechanics is to unify various laws from different areas of physics, such as fluid mechanics and solid mechanics. The same objective was also pursued by continuum mechanics, but the latter has not been entirely successful in accomplishing it. The Galilean invariance and the principle of equivalence make it possible to rewrite the law of dynamics as an equality between accelerations, the one undergone by the medium and the external accelerations applied to it. The derivation of the equation of discrete motion leads to writing the acceleration as a Hodge-Helmholtz decomposition, *i.e.* the sum of a gradient of a scalar potential and the rotational of a vector potential. By choosing the acceleration as being a primary variable, we can express the velocity and the displacement simply as quantities that accumulate over time. Potentials represent energies per unit mass and are also stored over time. The resulting formulation is able to describe the motion and dynamics of complex media, that can be both fluid and solid, under large deformations and large displacements. Two examples of fluid-structure coupling, an analytical solution and a numerical solution used for a benchmark, are presented here. They show the ability of the model to reproduce the behavior of interacting fluid and solid media.

## 1 Introduction

The continuum mechanics is supposed to unify the mechanics of both solid and fluids. Most of the numerous differences between these two mechanical modelings result in the fact that the equation of motion is not the same for them, for example the Navier-Stokes equation are formulated in terms of velocity in fluids whereas the Navier-Lamé equation are expressed in displacement in solids. Multiple differences between the two domains, fluid and solid, are related to one of the principal cause, the annexation of the conservation of mass to the Navier-Stokes equations. In fact, the initial decoupling between velocity and pressure requires the use of the law of mass conservation whatever the chosen coupling way between pressure and velocity. In fact, number of difficulties make this unification impossible in the concept of continuous medium [5].

Discrete mechanics differs in particular in that it does not require the use of tensors: the notion of vector itself is associated with a constant scalar on an oriented edge. The

concept of tensor introduced in the 18<sup>th</sup> century has made it possible to synthesize the normal and tangential stresses within the same operator applied to second-order tensors; if it is necessary for the Navier-Stokes equation to express the local deformation rate according to variable properties, it proves useless for the Navier-Lamé equation in rotational formulation. This is an original confusion between the tensor properties of anisotropic media and the formulation of the equation of motion. Although it is possible to use the tensorial form, it is not strictly necessary.

Multiple difficulties and artifacts still enameled the conservation laws for fluid and solid media. In fluids, the hypothesis of Stokes that  $3\lambda + 2\mu = 0$  is wrong [8, 11]. Even putting aside the Stokes hypothesis, the continuum mechanics consider for an isotropic medium that the tensor of elasticity of the fourth order  $\mathbf{C}$  is reduced to the two Lamé coefficients, these are conditioned by the Clausius-Duhem  $3\lambda + 2\mu \geq 0$  inequality that can potentially define a negative viscosity. In solids, the use of tensors leads to the writing of compatibility conditions to link constraints to displacements.

The discrete mechanics [5] proceeds from another vision, relying on the fact that vector quantities are assigned to a finite-length bipoint saving the direction in any homothetic reduction. A vector, velocity for example, will be a constant scalar attached to this oriented segment. The derivation of the equation of discrete motion is initiated from two principles emitted by Galileo, the relativity of motion and the principle of equivalence between masses associated with gravity and inertia. The fundamental law of the dynamics established in terms of forces by I. Newton then becomes an equality between accelerations, namely the acceleration undergone by a medium is the sum of the accelerations applied to it. This conservation law of the acceleration leads to express conservation equations in terms of velocities for the fluids but also for the solids. The principle of constraint accumulation makes it possible to derive accelerations relative to inertia, diffusion, dissipation and all the other forces per unit of mass which contribute to modify movement, gravitation, capillary effects, etc.

The equation of discrete motion is representative of all phenomena observed in fluid flows, solids with complex constitutive laws representative of large displacements and large deformations as well as the propagation of linear waves or shock waves. In classical cases with constant material properties, it allows to recover all the solutions obtained previously with the Navier-Stokes and Navier-Lamé equations.

## 2 Bases of Discrete Mechanics

### 2.1 Physical Model of Discrete Approach

Discrete mechanics is based on classical principles and postulates of physics; one of the most emblematic is the principle of equivalence introduced by Galileo that assigns an equivalent effect to the gravitational acceleration and the one due to inertia. This principle, now called the Weak Equivalence Principle (WEP), has been verified by numerous experiments quantified by the Eötvös ratio  $\eta = 2 |\gamma_1 - \gamma_2| / |\gamma_1 + \gamma_2|$  where  $\gamma_1$  and  $\gamma_2$  are the accelerations of the two masses. The measurement of the acceleration is independent of any reference and can be achieved with an absolute precision. The current state leads to estimating that the WEP is exact with a ratio of Eötvös  $\eta < 10^{-17}$ ; Will's [13] review cites the various experiments carried out for a century.

For gravitational effects only, this principle makes it possible to eliminate the mass of Newton's second law in order to obtain equality between the acceleration of the medium and the gravitational acceleration. In fact the fundamental law of dynamics in a more modern form  $\rho \boldsymbol{\gamma} = \mathbf{f}$  where  $\mathbf{f}$  is the sum of the volume forces applied to the medium is modified in discrete mechanics as follows:

$$\boldsymbol{\gamma} = \mathbf{g} \quad (1)$$

where  $\mathbf{g}$ , the sum of the forces per unit mass, is an acceleration.

By dissecting all the physical quantities and associated units by which they are expressed, it can be noticed that each time the mass appears in these units, this is only with a first order. It is therefore possible to define equivalent quantities but per unit mass. It appears that only two fundamental units, *i.e.* a length and a time, are required to quantify any physical variable.

Thus the notion of velocity  $\mathbf{V}$  is degraded, this one appears as a secondary variable whose value in absolute does not need to be known, it will not be present as such in the system of equations. The acceleration  $\boldsymbol{\gamma}$  takes on the contrary a fundamental status. It will be considered as an absolute quantity which can be measured in any place and at any moment. It possesses the essential property of satisfying the rule of vector summation, which is not the case with velocity, in any case for velocities close to the speed of light. The principle of relativity, also understood by Galileo, is therefore satisfied from the outset. A uniform translational motion is thus completely impaired in the equation of the discrete motion as the velocity appears only through discrete operators that filter this contribution. This is a little more complex for uniform rotation movements [5]. However at the end, these motions are also filtered by the same operators. These two stiffening movements have no effect on the acceleration of the particle or the material medium.

Another foundation of discrete mechanics is the Hodge-Helmholtz decomposition, see [1]. It establishes that every vector is the sum of a solenoidal component with null divergence and another irrotational one. A third component is sometimes associated, of harmonic type, being at the same time divergence and rotational free or constant. The vector is thus the sum of a gradient of a scalar potential  $\phi$  and a rotational of a vector potential  $\boldsymbol{\psi}$ . These are only defined to harmonic functions, the decomposition is not unique and depends on the boundary conditions. There are many potentials in physics and not all of them have the same importance. In discrete mechanics the vector considered is the acceleration  $\boldsymbol{\gamma}$ , an absolute quantity in a local reference frame. It is written naturally:

$$\boldsymbol{\gamma} = -\nabla\phi + \nabla \times \boldsymbol{\psi} \quad (2)$$

The harmonic term sometimes added is absent from this decomposition, it physically represents the movements of rectilinear translation and uniform rotation which disappear by application of the discrete operators. All undulatory physics are implicitly based on this relation: the terms of the right hand side are derived from orthogonal fields. The gradient and dual rotational operators project these fields on the same  $\Gamma$  edge and the sum of these two contributions is the acceleration applied to the medium. For example, in electromagnetism, the electric and magnetic fields  $\mathbf{E}$  and  $\mathbf{B}$  are orthogonal

to each other at any moment and themselves orthogonal to the wave vector  $\mathbf{k}_0$ . Thus a current can be applied from a potential difference or produced by induction from a magnetic field. The unification of the laws of macroscopic physics is thus considered under the undulatory point of view for any phenomenon of any nature, mechanical, acoustic, electrical, magnetic, optical [10].

## 2.2 Geometrical Topologies and Definitions

The notion of continuous medium is abandoned, as is that of global reference frame. There is a local discrete geometrical structure represented in Fig. 1 composed of primal and dual elementary structures. The term discrete geometric structure or geometric topology defines a set of links between connected elementary objects, here points, segments, surfaces. These notions are identical to those that can be found in mesh structures, for example resulting from spatial discretization in finite elements. The segment  $\Gamma$  of unit vector oriented  $\mathbf{t}$  and of ends  $a$  and  $b$  defines the basic element of the primal topology which, with two other segments, forms the planar surface  $\mathcal{S}$  whose unit-oriented normal is  $\mathbf{n}$  such that  $\mathbf{t} \cdot \mathbf{n} = 0$  (Fig. 1(a)). The scalar potential  $\phi$  is only defined at the ends of the primal topology. A possible contact discontinuity or shock wave  $\Sigma$  intersects the segment  $\Gamma$  into  $c$ . The normal to the  $\mathcal{S}$  plane is associated with a pseudo-vector  $\boldsymbol{\psi}$  such that the rotation of vector  $\mathbf{V}$  is itself associated with the segment  $\Gamma$ . Figure 1(b) represents the primal surface  $\mathcal{S}$  as a planar polygon; the  $\delta$  outline and the  $\Delta$  surface form the dual topology. The material medium, a flux of particles or an isolated particle represented by a  $p$  sphere in Fig. 1(a) has a velocity and a spin but only their components are explicitly represented on each  $\Gamma$  segment.

The thus defined primal and dual topologies intrinsically satisfy two essential discrete properties  $\nabla_h \times \nabla_h \phi = 0$  and  $\nabla_h \cdot (\nabla_h \times \boldsymbol{\psi}) = 0$ . They are verified whatever the topologies based on planar surfaces, polygons or polyhedra and whatever the regular functions  $\phi$  and  $\boldsymbol{\psi}$ . These conditions are absolutely necessary for a complete Hodge-Helmholtz decomposition applied here to acceleration. Each vector can be decomposed into a solenoidal part and an irrotational component, but the scalar and vectorial potentials are not of the same importance according to the nature of the vector.

It should be noted that  $\phi^o$  and  $\boldsymbol{\psi}^o$  are the stresses at time  $t$ , *i.e.* all the forces applied before this instant are “remembered” and stored. The formalism presented here enables us to take into account the entire history of the medium, *i.e.* its evolution over time from an initial neutral state. For a given instantaneous state of strain, there may be multiple paths by which this state can be reached, and  $(\phi^o, \boldsymbol{\psi}^o)$  will, alone, contain the whole of the medium’s history. It is not helpful to know the local and instantaneous stresses, in that these two potentials will have accumulated stresses over time. These quantities are also called “accumulators” or “storage potentials”. These potentials can therefore be used to take into account the behavior of media with continuous memory.

## 2.3 Discrete Motion Equation

The discrete motion equation is derived from the conservation equation of acceleration (2) by expressing the deviations of potentials  $\phi$  and  $\boldsymbol{\psi}$  as a function of velocity  $\mathbf{V}$ . These “deviators” are obtained on the basis of the physical analysis of the storage-release

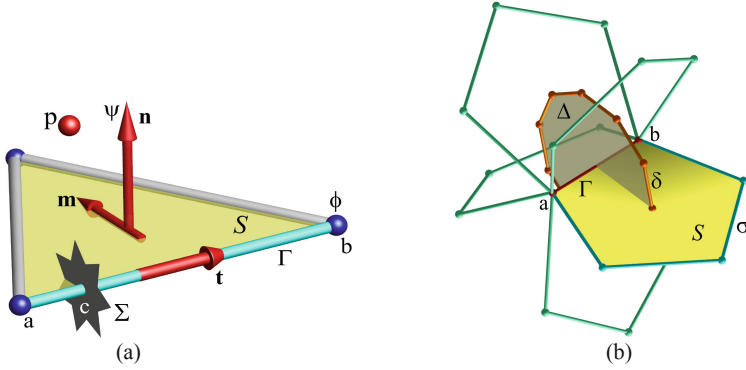


**Fig. 1.** (a) Elementary geometrical structure of discrete media mechanics in direct referential  $(\mathbf{m}, \mathbf{n}, \mathbf{t})$ : three straight  $\Gamma$  edges delimited by dots define a planar face  $\mathcal{S}$ . The unit normal vectors  $\mathbf{n}$  to the face and the vector carried by  $\Gamma$  are orthogonal,  $\mathbf{t} \cdot \mathbf{n} = 0$ . The edge  $\Gamma$  can be intercepted by a discontinuity  $\Sigma$  located in  $c$ , between the ends  $a$  and  $b$  of  $\Gamma$ .  $\phi$  and  $\boldsymbol{\psi}$  are the scalar and vector potentials respectively. (b) The virtual machine of motion in Discrete Mechanics: the acceleration of the medium along the edge  $\Gamma$  is due to the difference of the scalar potential  $\phi$  between the ends of the edge  $[a, b]$  of unit vector  $\mathbf{t}$ , to the circulation action of the vector  $\mathbf{V}$  on the contour of the different primal facets  $\mathcal{S}$  inducing an acceleration on  $\Gamma$  and the projection  $\mathbf{g} \cdot \mathbf{t}$  imposed other accelerations as gravity. The particle  $p$  has a velocity and an acceleration whose projections on the  $\Gamma$  edges are named respectively  $\boldsymbol{\gamma}$  and  $\mathbf{V}$ .

processes of compression and shear energies. The first is written as the divergence of velocity and the second as a dual rotational velocity. The physical modeling of these terms is developed in a book devoted to discrete mechanics [5].

The vectorial equation of movement and its upgrades are written as:

$$\left\{ \begin{array}{l} \boldsymbol{\gamma} = -\nabla(\phi^o - dt c_l^2 \nabla \cdot \mathbf{V}) + \nabla \times (\boldsymbol{\psi}^o - dt c_t^2 \nabla \times \mathbf{V}) + \mathbf{g} \\ \alpha_l \phi^o - dt c_l^2 \nabla \cdot \mathbf{V} \mapsto \phi^o \\ \alpha_t \boldsymbol{\psi}^o - dt c_t^2 \nabla \times \mathbf{V} \mapsto \boldsymbol{\psi}^o \\ \mathbf{V}^o + \boldsymbol{\gamma} dt \mapsto \mathbf{V} \end{array} \right. \quad (3)$$

The quantities  $\phi^o$  and  $\boldsymbol{\psi}^o$  are the equilibrium potentials, the same ones that allow the equation to be satisfied exactly at the discrete instants  $t$  and  $t + dt$ .  $c_l$  and  $c_t$  are the longitudinal and transverse celerities, intrinsic quantities in the medium that can vary according to physical parameters. The terms  $dt c_l^2 \nabla \cdot \mathbf{V}$  and  $dt c_t^2 \nabla \times \mathbf{V}$  are respectively the deviators of the compression and shear effects. The second member is thus composed of two oscillators in which  $\phi^o$  and  $\boldsymbol{\psi}^o$ , which represent energies per unit mass, exchange these energies with their respective deviators. The two terms in gradient and in dual rotational are orthogonal and can not exchange energy directly. If an imbalance due to an external event occurs on one of these effects, acceleration is modified and energy is then redistributed towards the other term. The acceleration  $\mathbf{g}$  represents gravity or

any other source quantity and will also be written in the form of a Hodge-Helmholtz decomposition.

The physical parameters  $\alpha_l$  and  $\alpha_t$  are the attenuation factors of the compression and shear waves. They also depend only on the considered medium: for example, a Newtonian fluid retains the shear stresses only for very weak relaxation time constants, of order of magnitude of  $10^{-12}$  s and the coefficient  $\alpha_t$  can be taken as zero. The updating of potentials at time  $t + dt$  is thus affected by these coefficients ranging from zero to unity. The velocity and possibly the displacement  $\mathbf{U}$  are also upgraded. In the case where the density is not constant, it is also updated using the conservation of mass in the form  $\rho = \rho^o - dt \rho^o \nabla \cdot \mathbf{V}$ . This quantity is only a function of the divergence of velocity.

The acceleration  $\boldsymbol{\gamma}$  and the particle derivative of the velocity are written as  $\partial \mathbf{V} / \partial t + \mathbf{V} \cdot \nabla \mathbf{V}$  or using the Lamb vector  $\partial \mathbf{V} / \partial t - \mathbf{V} \times \nabla \times \mathbf{V} + \nabla (\|\mathbf{V}\|^2 / 2)$  in continuum mechanics. These expressions can not be transformed into a Hodge-Helmholtz decomposition, the notion of tensor being non-existent in discrete mechanics. Similarly, the Lamb term is not a rotational one. The acceleration is thus rewritten in the form of irrotational and solenoidal components of a Hodge-Helmholtz decomposition of inertial potential  $\phi_i = \|\mathbf{V}\|^2 / 2$ . All other source terms applied to the medium or particle can also be written as a Hodge-Helmholtz decomposition.

### 3 Validation of the DM Model

The formulation of discrete mechanics makes it possible to find all the results obtained with the Navier-Stokes equation in the case of a medium with constant properties, mainly the density, the viscosity and the coefficient of compressibility (or the celerity of the waves). In the case where the properties are variable in space, the formulations differ.

The exact solutions of the Navier-Stokes equations corresponding to physical cases such as the Poiseuille or Couette flows are also exact solutions of the equation of discrete mechanics when these solutions are formulated in the form of polynomials of degree equal to or less than two. In the case of any continuous functions, the numerical solution obtained by the discrete formulation proves orders of convergence in time and in space equal to two. This is for example the case of the synthetic solution of the Green-Taylor vortex. Simulations of simple constraints applied to solids, compression, bending, torsion make it possible to find the theoretical solutions also. Benchmarks on fluid-structure interactions [3,4], compare very favorably with solutions obtained by other authors.

The few validation cases presented here make it possible to confirm that the Navier-Stokes equation and the discrete mechanics have the same solutions but above all, to show the versatility of the latter unifying the representation of fluid flows, of complex materials behaviors in an unsteady unified approach.

#### 3.1 Oscillatory Fluid-Solid Interaction

Even if the rheology of the medium is more complex, e.g. viscoelastic fluids, non-linear viscosity laws, viscoplastic fluids, time-dependent properties, and so on, we should still

be able to represent its behavior under various types of applied stress. In some cases, the shear-rotation stresses may only be partially accumulated. We can describe viscoelastic behavior by weighting the accumulation term of  $\boldsymbol{\Psi}^o$  by an accumulation factor  $0 \leq \alpha_t \leq 1$ . Fluids with thresholds can also easily be represented by specifying a value of  $\boldsymbol{\Psi}^o = \boldsymbol{\Psi}_c$  below which the medium behaves like an elastic solid. Many of the difficulties that are typically encountered in rheologies with non-linear viscosities are no longer an issue with DM.

In discrete mechanics, the concepts of viscosity and shear-rotation are exclusively associated with the faces of the primal topology, where the stress may be expressed in the form  $\mathbf{v} \nabla \times \mathbf{V}$  in fluids and  $dt \mathbf{v} \nabla \times \mathbf{V}$  in solids. As an example, let us consider the interaction between an incompressible viscous Newtonian fluid and a neo-Hookean elastic solid. The stress tensor of an incompressible isotropic hyperelastic material is as follows in the neo-Hookean model:

$$\boldsymbol{\sigma}_s = -p \mathbf{I} + \mu_s \mathbf{B}, \quad (4)$$

where  $\mathbf{B} = \mathbf{F}\mathbf{F}^T$  is the left Cauchy-Green deformation tensor. In two spatial dimensions, the Cayley-Hamilton theorem can be used to show that the Mooney-Rivlin model of a hyperelastic material is equivalent to the neo-Hookean model.

We shall study a problem that was published by Sugiyama in 2011 [12]. Consider an elastic band with an applied shear stress generated by the periodic flow of an incompressible Newtonian fluid. The flow is laminar and periodic in  $x$ . Given that there are no compression terms, we can solve the problem in one spatial dimension along the  $y$ -axis for  $y \in [0, 1]$ . Suppose that the upper interface follows the periodic motion  $V(t) = V_0 \sin(\omega t)$ , where  $V_0 = 1$  and  $\omega = \pi$ . The velocity of the lower surface is imposed at zero. The solid occupies the lower part of the domain, and the fluid occupies the upper part of the domain; the position of the interface is  $y = 1/2$ . The theoretical solution found by Sugiyama was obtained by separating the spatial variable  $y$  from the time variable  $t$ . A homogeneous solution is found by considering a basis of Fourier functions on the interval  $y \in [0, 1]$  and exponential functions on the time interval in each of the fluid and solid domains separately. The sequence of Fourier coefficients can be determined from the coupling at the interface by requiring the velocity and the stress to be continuous.

We can find a solution  $V(y, t)$  directly from the equations of discrete mechanics [1] simply by imposing the relevant conditions at  $y = 0$  and  $y = 1$ . The coupling conditions at the interface, namely the continuity of the velocity and the stress, are implicitly guaranteed to hold by the dual curl operator. The notion of a 2D or 3D space does not exist in discrete mechanics. Instead, the operators define the orientations of the normal and tangent directions within a three-dimensional space. Despite this, the assumptions made in this example enable us to solve along a single spatial dimension. The time step is chosen to be  $\delta t = 10^{-4}$  to ensure good overall levels of accuracy. By comparing against the theoretical analytic solution, it can be shown that the numerical solution is second-order in space and time.

Figure 2 plots the velocity and the displacement of the interface  $\Sigma$  over time. The velocity of the upper wall is also shown. The solution establishes itself very quickly. After just a few periods, the velocity becomes fully periodic. The velocity profiles are

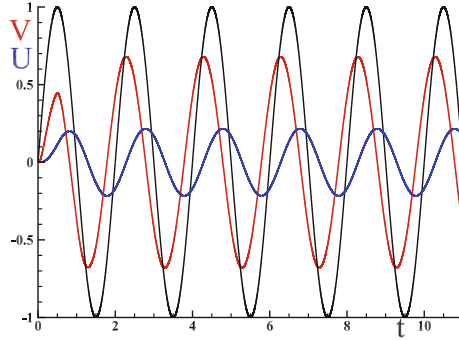


**Fig. 2.** Study of a periodic fluid-structure interaction between a viscous fluid and an elastic solid. The kinematic viscosity of the fluid is  $\nu = 1$  and the shear modulus of the solid is  $\nu = 4$ . The velocity of the fluid at the upper wall is shown in black, the velocity of the interface  $\Sigma$  is shown in red, and the displacement over time of the solid  $U$  at the interface is shown in blue.

shown until  $t = 10$ . The displacement of the solid over time may be deduced from the relation  $\mathbf{U} = \mathbf{U}^o + \mathbf{V} dt$ , where  $dt$  represents both the differential element and the time increment  $\delta t = dt$ . Note that the displacement is strongly out of phase with the velocity of the interface.

A selection of the velocity profiles in the  $y$ -direction are shown in Fig. 3 once the periodic regime is fully established. The results converge to second order in space and time. Given the absolute accuracy (of the order of  $10^{-4}$  s) obtained using a coarse mesh ( $n = 32$ ), we can conclude that there is no observable error between the theoretical solution and the numerical solution.

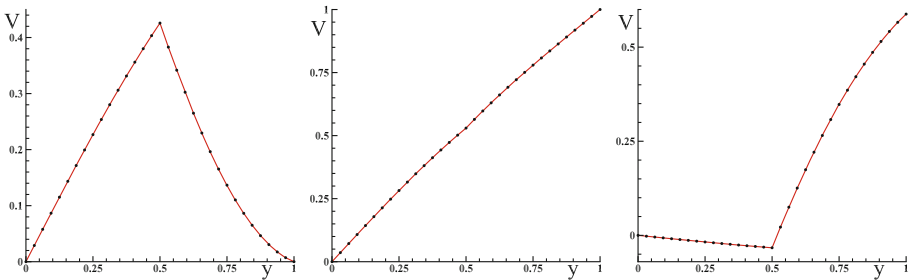


**Fig. 3.** Study of a periodic fluid-structure interaction between a viscous fluid and an elastic solid. The viscosity of the fluid is  $\nu = 1$  and the shear modulus of the solid is  $\nu = 4$ . The figures show the velocity profiles as a function of  $y$  at time  $t = 10$ ,  $t = 10.5$ ,  $t = 10.8$ . The solid line holds for the theoretical solution whereas the points represent the spatial approximation obtained with 32 cells.

One advantage of the fluid-structure interaction for a neo-Hookean model described by Sugiyama is that it has a theoretical solution. This allows us to compare the numeri-

cal solutions that we obtain more precisely, but also allows us to develop new concepts, as we did for discrete mechanics in this section. Sugiyama obtained a first-order error in the  $L_2$  and  $L_\infty$  norms, whereas the model [1] achieves second-order results with much lower absolute errors. This improvement is ultimately attributable to the separation of the properties at the interface, as well as the fact that no interpolation is performed, despite a fully monolithic and implicit treatment of the fluid-solid coupling.

Fluid-structure interactions in 2D or 3D geometries with a moving interface can of course also be solved using the system [1]. However, without an analytic solution for comparison, there is little benefit in doing so, since the errors of the various methodologies accumulate over each step of the process. Other more complex constitutive laws can also be modeled.

### 3.2 Lid-Driven Open Cavity Flow with Flexible Bottom Wall

The lid-driven cavity with flexible bottom is an example that we can reasonable deal with. This case corresponds to that proposed in reference [9]. It was also considered by others authors [2,6]. A fluid, characterized by density  $\rho_f = 1 \text{ kg m}^{-3}$  and viscosity  $\mu = 10^{-2} \text{ Pa.s}$ , is driven by the velocity boundary condition of the top of the cavity which varies with time:  $u(x,t) = 1 - \cos(2\pi t/T)$ , where the period is equal to  $T = 5 \text{ s}$ .

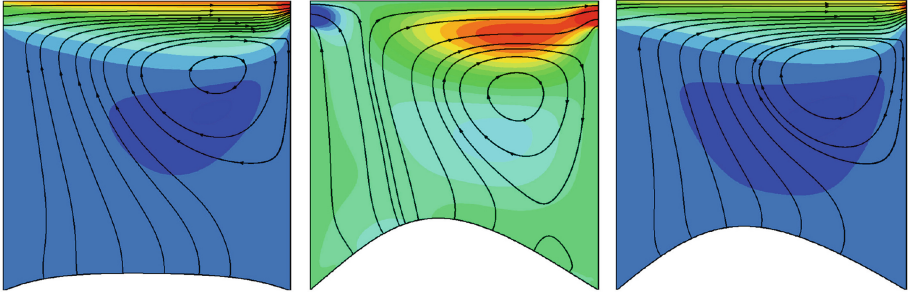


**Fig. 4.** Lid-driven open cavity flow with flexible bottom wall, velocity and streamlines at  $t = 2.5, 15, 20 \text{ s}$ .

The elastic structure density is  $\rho_s = 500 \text{ kg m}^{-3}$ , the Young modulus is  $E = 250 \text{ Pa}$  and the Poisson coefficient  $\sigma = 0$ . The fluid is considered as incompressible. Neumann boundary conditions are imposed on the two holes localized at the top of the vertical walls. As we resolve at the same time, the velocity field and the displacement field in the fluid and the elastic membrane respectively, using a fixed grid, we have to take a relative large thickness for the membrane (2% of the cavity length) compared to other simulations of the literature, in order to prevent using a very fine grid. A one dimensional deformation of the membrane can be dealt using another numerical scheme. The formulation and the equations used are that proposed in the article. Only the procedure

related to the membrane deformation and the numerical scheme are different. The differential discrete operators, such as gradient, divergence and rotational properties have the properties of continuum  $\nabla \cdot \nabla \times \boldsymbol{\psi} = 0$  and  $\nabla \times \nabla \phi = 0$  on every type of unstructured polyhedral meshes. This methodology is close the Discrete Exterior Calculus one [7]. In the present case, adaptive quadrangle mesh is used with initially 2562 cells. The resolution of the motion equation of the fluid allows to obtain the pressure on the top surface of the membrane, the lower surface being maintained at a constant pressure  $p = 0$ . The force acting on the membrane, proportional to the pressure difference, allows to calculate its displacement. The mesh is then modified and this at each time steps. This is what we call the Arbitrary Lagrangian Eulerian method.

The results obtained are presented in the Fig. 4 where the horizontal velocity maps in the fluid and the membrane shape are shown together with the streamlines for different time steps.

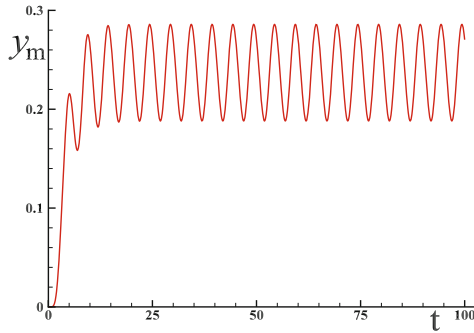


**Fig. 5.** Lid-driven open cavity flow with flexible bottom wall. Evolution of maximum deviation of membrane  $y_m$  over time.

These results are in good agreement with those of [2] and [6]. After an unsteady phase of a few cycles, the regime becomes totally periodic, of period  $T = 5$  s (Fig. 5). The divergence of the velocity remains less than  $10^{-8}$  throughout the calculation. The celerity of air, which is equal to  $c \approx 340 \text{ms}^{-1}$ , maintains the flow in the incompressibility approximation for the selected time period  $dt = 10^{-2}$  s. Indeed the discrete model clearly shows that the Mach number  $M = v/c$  does not define the incompressibility of a flow: this is the product  $dt c_l^2$ . For example water, an essentially incompressible fluid, propagates the waves at a celerity of  $c_l \approx 1500 \text{ms}^{-1}$  which induces the fact that water is a compressible medium if the observation time constant  $dt$  is sufficiently low.

## 4 Towards a Unification of Solid and Fluid Mechanics

The most significant achievements of the discrete approach are as follows:

- discrete mechanics proposes a unique formulation of the equations of motion in terms of the velocity to represent the motion of both fluids and solids;

- the velocity variable, the displacement, and the stresses ( $p^o, \boldsymbol{\omega}^o$ ) or ( $\phi^o = p^o/\rho, \boldsymbol{\psi}^o = \boldsymbol{\omega}^o/\rho$ ) are calculated simultaneously and accumulated by simple differential operators;
- the accumulation process for the stress holds for large displacements and large deformations.

This theory describes the motion and displacements of solids and fluids consistently, but the scope of the proposed description also extends to the dynamic behavior of these materials and the propagation of waves within them. Possibly, the most important result of discrete mechanics for fluids and solids is the formal Hodge-Helmholtz decomposition of the equations of motion. The decomposition into irrotational and solenoidal components enables us to understand the mechanisms governing the equilibrium of a medium, and the divergence and curl of the velocity can be used to deduce the stresses, namely the equilibrium pressure  $p^o$  and the rotation stress  $\boldsymbol{\omega}^o$ .

## References

1. Angot, Ph., Caltagirone, J.-P. and Fabrie, P.: Fast discrete Helmholtz-Hodge decomposition in bounded domains. *Appl. Math. Lett.* **26**(4), 445–451 (2013)
2. Bathe, K.-J., Zhang, H.: A mesh adaptivity procedure for CFD and fluid-structure interactions. *Comput. Struct.* **87**, 604–617 (2009)
3. Bordère, S., Caltagirone, J.-P.: A unifying model for fluid flow and elastic solid deformation: a novel approach for fluid structure interaction. *J. Fluid Struct.* **51**, 344–353 (2014)
4. Bordère, S., Caltagirone, J.-P.: A multi-physics and multi-time scale approach for modeling fluid-solid interaction and heat transfer. *Comput. Struct.* **164**, 38–52 (2016)
5. Caltagirone, J.-P.: *Discrete Mechanics, Concepts and Applications*, ISTE. Wiley, London (2018)
6. Kassiotis, C., Ibrahimbegovic, A., Niekamp, R., Matthies, H.: Nonlinear fluid-structure problem, part I: implicit partitioned algorithm, nonlinear stability proof and validation examples. *Comput. Mech.* **47**, 305–323 (2011)
7. Desbrun, M., Hirani, A.N., Leok, M., Marsden, J.E.: Discrete exterior calculus. *arXiv-math/0508341v2*, pp. 1–53 (2005)
8. Gad-El-Hak, M.: Stokes hypothesis for a Newtonian, isotropic fluid. *J. Fluids Eng.* **117**, 3–5 (1995)
9. Gerbeau, J.F., Vidrascu, M.: A quasi-Newton algorithm based on a reduced model for fluid-structure interaction problems in blood flows. *Math. Modell. Numer. Anal.* **37**, 3–5 (2003)
10. Marsden, J.E., Ratiu, T., Abraham, R.: *Manifolds, Tensor Analysis, and Applications*, 3rd edn. Springer, New York (2002)
11. Rajagopal, K.R.: A new development and interpretation of the Navier-Stokes fluid which reveals why the “Stokes assumption” is inapt. *Int. J. Non-Linear Mech.* **50**, 141–151 (2013)
12. Sugiyama, K., Ii, S., Takeuchi, S., Takagi, S., Matsumoto, Y.: A full Eulerian finite difference approach for solving fluid-structure coupling problems. *J. Comput. Phys.* **230**, 596–627 (2011)
13. Will, C.M.: The confrontation between general relativity and experiment. *Space Sci. Rev.* **148**, 3–13 (2009)



# HPC and Data: When Two Becomes One

Christophe Calvin<sup>(✉)</sup> and France Boillod-Cerneux

CEA Saclay, DRF, Gif Sur Yvette, France  
{christophe.calvin, france.boillod-cerneux}@cea.fr

**Abstract.** As claimed for many years, High Performance Computing (HPC) and high performance numerical simulation are necessary tools for fundamental science and engineering. Big data and artificial intelligence are some newcomers in the landscape, but not that new, especially in science. Finally, open data and open science are becoming now mandatory for trustable and reproducible science.

This paper presents the recent evolution of HPC with the spectacular arising of AI. HPC and AI share at least one common point: Data. Many HPC communities are struggling with data, whether they are coming from simulation and wait to be analyzed, or coming from large instruments (experiments, observatories) and wait to be treated.

Data was not a major focus in the last decades for HPC community but it reshapes HPC paradigms by introducing data as a “scientific pillar”.

We will first present the current HPC context and how AI changed the current HPC landscape. We will then focus about data use in HPC and how AI can improve HPC simulations. We will also present the concept of FAIR data and why this concern shall be treated soon and embraced by HPC and AI community. We will finally conclude on the data issue and present our point of view regarding the future evolution of HPC market.

**Keywords:** HPC · AI · Open Science · Data

## 1 Introduction

With exascale challenge, Top500 [1] has really mutated, either regarding the supercomputers listed and regarding its weight to estimate a supercomputer’s compute power.

The first mutation comes from the exascale challenge itself. Power wall is hard to cross and so far, (safe) decision has been made to promote low consumption processors or high multicore processors while trying to keep a reasonable power consumption of the overall machine.

Top500 is heckled by new rankings, such as Green500 [3] that proposes to classify supercomputers by Flops per Watts rather than just Flops/s capacities. This rank strategy deeply reshapes the Top500 ranking, as very few of the top 10 coming from Top500 can reach Green500 first ranks. Green500 also emphasizes

Japan's effort to build low energy consumption machines, as 6 over 10 of the best Green500 machines come from Japan.

HPCG500 (High Performance Conjugate Gradients) [4] is either getting more and more attention from HPC community: Indeed, Linpack benchmark for Top500 provides an efficiency from 50% to 80% from peak compute capacity, while real users applications have about 10% efficiency from peak performance. Few of real applications can address the compute bound profile of High Performance Linpack (HPL): In this context, HPCG is raised as a "more representative" benchmark, closer to "real HPC applications" profile. It is not surprising to see that HPCG500 and Top500 present very different ranking, but the difference is less striking than Green500. However, if we compare the HPL peak performance and HPCG peak performance, then the reality of supercomputer compute capacity becomes closer to reality.

Even though the change is unavoidable, it is either not quite smooth. Last petaflop homogeneous supercomputers propose mostly massive parallel processors, and users must take care of their application parallelism (especially multi-level parallelism) if they really want to see a performance gain on the last petaflop computers.

On the other side, Top500 is fastly tainted by hybrid architecture (classic processors with accelerators such as Graphic Process Units), which is a direct consequence of exascale power wall. NVIDIA<sup>®</sup> GPUs strike hard the 2018 Top500: Half of top 10 most powerful supercomputers (November 2018 Top500 list [2]) contains nodes with NVIDIA<sup>®</sup> GPUs. However, taking full advantage of hybrid nodes efficiency requires large effort for HPC community. Choosing GPUs acceleration is mostly a tradeoff portability versus efficiency (in terms of compute power and energy consumption). This trend is justified by the excellent ratio of Flops per Watts of NVIDIA<sup>®</sup> GPUs but also by the ongoing evolution (that is actually not far from a revolution) of HPC landscape.

"Hybrid" word must be used with caution: indeed, we traditionally referred to hybrid architecture as compute nodes with accelerators (such as GPUs), but hybrid may now, depending on the context, refer to the community addressed by the supercomputer. Looking closely at the top 10 of the Top500 November 2018 list, we observe that 2 of them, Summit (USA) and ABCI (Japan) clearly expose their membership to AI research: That is to say, Summit and ABCI are not HPC dedicated but at the best, AI dedicated and at the worst, HPC and AI dedicated. This recent trend is likely to be spread to the other Top500 computers and might contaminate very quickly the full Top500.

The fusion of HPC and AI is clearly illustrated by many HPC centers that are enlarging their scope of action: As an example, Argonne Leadership Computing Facility (ALCF) from Argonne National Laboratory (ANL) has officially announced the integration of Machine and Deep Learning as one of their scientific pillars. Most of the historic and HPC actors made similar declarations.

In what follows we will focus on how AI reshapes the HPC community and can help to consider data as a key point in their simulation process. We will then

focus on the data issue, and address the FAIR data concept, which may lead in the future both HPC and AI scientific research.

## 2 HPC (R)evolution

### 2.1 When AI Shakes HPC

Since the end of 2018, many HPC media relay the announcements of supercomputers dedicated to AI as well as strong positions to promote AI science and development. The recent appearance and success of Deep500 [5], the ranking of most powerful computers dedicated to AI (or HPC and AI) is a very good illustration of Machine and Deep Learning success in industry and scientific fields.

**AI Adoption.** The Deep Learning (DL) success can be attributed to enterprises and industries who have massively used it to improve their process, or wisely address their (future) customers. Deep learning is currently widely adopted by public at large scale. This might be seen as a very “late recognition” as AI discipline was born many decades ago, around 1950. Success of AI and more specifically Deep Learning is largely due to the GAFAM (Google, Apple, Amazon, Facebook and Microsoft) but not only. At a more global scale, in the last decades, every industry, every organization and everyone has gathered massive amount of data. The convergence of a large amount of data and the maturity of available computing hardware drove AI from “theoretical” discipline to “executable” discipline, and currently, “unavoidable” discipline.

**AI and HPC Fusion.** Deep Learning is driven by data and HPC is generating huge amount of data. Therefore, it is not very surprising to observe the collision of these two disciplines. On another level, HPC community is quite mature now and organized. It has access to a large panel of HPC platforms, addressing many different needs in terms of hardware and compute capacity needs. The progression of AI inside the HPC community is coming from four needs:

- AI needs large platforms to run specific experimentations, and HPC can offer such platforms,
- HPC is struggling with data and their analyses,
- Many HPC applications cannot cross petaflop or exaflop scale due to their algorithms and/or the physics model and numeric used,
- Governments have identified AI as a strategic point, at least as important as HPC.

**AI Supercomputers Might Cross Exascale First.** Machine Learning and Deep Learning completely reshape exascale challenge thanks to their ability to reduce the compute precision. Though many HPC simulations require a fine precision, Machine Learning and Deep Learning applications can be satisfied with very low precision.